International Journal of Sciences: Basic and Applied Research (IJSBAR)

ISSN 2307-4531
(Print & Online)

http://gssrr.org/index.php?journal=JournalOfBasicAndApplied

Experimental Investigation of Permeability Alteration Due to Drying of Porous Media

Monday Obekpa Michael[a*], Lobe David Nje[b]

[a.b]*Department of Petroleum Engineering, Khazar University, Baku, AZ1096, Azerbaijan*

[a]*Email: mondaymichael.12@gmail.com,* [b]*Email: lobe.david@khazar.org*

Abstract

The permeability of reservoir rocks can be significantly altered by the precipitation of brines caused by drying. In this study, alteration of permeability in porous media induced by drying of brines was investigated experimentally. Four different rock types were used; rock samples were initially analysed by X-ray diffraction (XRD) and conventional core analysis (CCAL), including gas permeability and Helium porosity. The reservoir rock samples (2 each of carbonate and sandstone) were tested to determine the impact of rock type and initial permeability on possible injectivity impairment. Each of the rock samples was completely saturated in brine of NaCl, KCl and Caspian seawater (SW), with salt concentrations ranging between 10 and 200 g/L. The samples were then fully dried in an oven at a controlled, constant temperature of 70^{o}C. The final gas permeability of each sample was measured after drying and compared with its initial value to determine the fractional permeability alteration. At the microscopic, pore-scale level, the extent of hindrance to flow from salt precipitation caused by drying of brines was investigated via scanning electron microscopy (SEM). The results indicate that the evaporation of aqueous brine occurs near the surface, and is controlled by convection current, evidenced by a Peclet number >>1.

Keywords: porous media; permeability alteration; precipitation; drying; greenhouse gases; carbon sequestration; saline aquifers.

---

* Corresponding author.

1. Introduction

According to the International Energy Agency (IEA) report on Global Energy and CO_2 Status Report for 2017, global energy-related CO_2 emissions grew by 1.4% in 2017, reaching a historically high value of 32.5 gigatons (Gt) [1]. This significantly high value of CO_2 emission from fossil fuels and other sources has led to vast amounts of time and effort being spent on research. Research into the ways and means of reducing the amount of greenhouse gases emitted into the atmosphere from natural and manmade processes has continued to attract attention. One very practical and successful method is geological sequestration of CO_2 into shallow and deep saline aquifers, which offers a very promising solution to reducing net global emissions of the gas into the atmosphere; the reasons being that these aquifers possess enormous storage capacities, high injectivity rates, and good containment to prevent leakage [2,3]. While this method may guarantee the continued use of fossil fuels with sustainable management of the emitted CO_2, it will however lead to an imbalance in the equilibrium of the physical and geochemical attributes of the host rock and aquifer. The most affected area of the aquifer is in the vicinity of the injection well. This area is particularly affected by the injection of supercritical CO_2 where chemical processes (such as mineral dissolution and precipitation), and physical processes (such as temperature, pressure and gravity) reduce reservoir rock porosity and permeability and consequently impact well injectivity [4].

The most significant and troublesome cause of imbalance in equilibrium is the drying of the porous media, with a wide range of implications ranging from salt precipitation [2], alteration of the local geomechanical constraints due to salt precipitation, modification of internal forces, and effect of injected fluids on the interfacial tensions (i.e., capillary/osmotic phenomena) [4]. When CO_2 (non-wetting phase) is injected into a porous media fully saturated with fluid (i.e., brine), the mobile water (wetting phase) is displaced by the supercritical, dry CO_2 while also causing evaporation simultaneously, a process known as *flow-through* drying. After injection of several pore volumes of the non-wetting phase, a significant fraction of the wetting liquid (water) remains immobilised, trapped in the pore space, or distributed on grain surface as a thin film, and is now in contact with the dry flowing CO_2. Therefore, a continuous and an elaborate evaporation process leads to the appearance of a drying front, which steadily moves into the medium (rock or aquifer), and the precipitation of salts and other minerals present in the brines [4]. The drying of a porous medium is a very important unit operation, with applications in diverse areas: environmental and industrial applications, such as groundwater and soil remediation, food processing and preservation, geological applications such as CO_2 storage, geothermal energy storage in hot aquifers; catalysts and fuel cell production, and recovery of hydrocarbons from underground reservoirs [5]. In these applications, there is the need to remove liquid from a solid porous matrix. The removal of water in porous media can be achieved through the continuous flow of a displacing phase. If the displacing phase is immiscible and incompressible, water is removed only by *forced* displacement. However, if the displacing phase is immiscible but compressible, water can be removed by evaporation due to expansion of the gas phase [6]. The effects of evaporation brought by the flow of a dry gas, such as nitrogen or carbon dioxide, have been studied extensively as far back as the mid-20th century by Allerton and his colleagues [7], where *flow-through drying* was studied using packed beds of crushed quartz and glass beads with injected dry gas phase at elevated temperatures. The evaporation regime comes into effect after the immiscible displacement of the initial solvent (water) by the injected gas. In contrast to diffusion-driven drying [8] where dry gas passes over the

external surface of a liquid saturated porous medium, theoretical and experimental studies into flow-through drying are limited, and therefore not well understood. Some of the earlier diffusion-driven drying theories were developed by Luikov [9], and Whitaker [10,11], which were based on volume averaging methods while assuming a constant gas pressure. Some recent studies have also been done, using numerical simulations, to evaluate the risk of salt deposition in underground geological storage. In these studies, the 2-phase Darcy models were used to determine the distribution of phases saturation over a period of time [3,12,13].

In all situations where there is need to remove water from a solid matrix, complex flows inside the many porous structure determines the dynamic of the drying process: capillary flow brings the water towards the surface of the porous medium, then diffusion of the water vapour transfers some part of the water, while adsorption/desorption of water film can limit the evaporation rate. This detailed overview of the drying mechanism has been presented by Nadeau and Puiggali in Ref. [14]. Furthermore, the evolution of the drying rate has also been studied extensively by a number of other researchers, which has led to the definition of the *drying rate* as mass of water loss per unit surface and per unit time [15], a parameter that is regularly recorded as mass over periods of time. In a homogenous medium, such as beads and sand packs, it is observed that the drying rate in the first period is constant, then followed by a fast decreasing rate period, and then another decreasing rate period at a much reduced rate [15]. In the first period, water inside of the porous structure is brought to the surface from where it evaporates via capillary force. In this period, the drying rate is supposedly constant, controlled by the diffusion of water vapour at the surface of the porous medium towards the exterior. In the next period, the decreasing period, starts when the water network breaks and the capillary force is not sufficient to drive the water to the porous medium surface. In this period, the drying rate decreases significantly. In the final period, the desaturation of the water is connected to the adsorption/desorption of the remaining water films and the drying rate becomes even weaker [15].

In a number of recent research works performed on this subject, particularly those with a focus on ion transport in evaporating systems, results obtained have showed the importance of a dimensionless parameter, the ***Peclet number***, *Pe*. The Peclet number, *Pe*, is computed, both at low and high evaporation rates, to determine the controlling process during evaporation in a saturated brine experiment. Peclet number, *Pe*, is computed from Equation (1):

$$Pe = \frac{hL}{D\emptyset_0} \dots\dots\dots\dots\dots\dots\dots (1)$$

Where h is drying rate in $m^3/m^2.s$ [= mean drying rate / (cross-sectional area x density of water)]; L is length of core plug in m; D is diffusion coefficient in m^2/s; $\emptyset_0$ is initial core plug porosity (dimensionless). For high Peclet numbers ($Pe>>1$), the salt accumulates at the evaporating surface, while for low Peclet numbers ($Pe<<1$), diffusion dominates, and the deposited salt profile is homogenous and spreads out in the rock matrix [5]; a cross-over behaviour between these 2 extremes occur when $Pe \approx 1$ [16]. Various one-dimensional (1D) results have been obtained from these studies, where nuclear magnetic resonance (NMR) measurements have corroborated some of the basic predictions [17], particularly those that combine moisture content with ion concentration profile near the drying interface.

In this work, the reduction in permeability caused by pore-clogging from brine precipitation induced by drying of reservoir rock samples using dry nitrogen gas is experimentally investigated. The dry gas flows through the core samples at an imposed injection pressure. The objective of this study was to permeability alteration caused by salt precipitation, which is induced by drying under controlled conditions of temperature and pressure; this trend in permeability reduction are then interpreted using the capillary tube model, and an alteration model produced consequently. In situations where the physical processes involved in the porous medium are not easily recognisable, imaging studies have been used to visualise the saturation profiles to understand regimes of displacement and evaporation [18,19]. In this work, we used SEM to investigate the type of flow-through drying mechanism observed in the core samples at a localised pore level.

2. Materials and Methodology

2.1 Rock Sample

Two categories of reservoir rock were used in this study, namely: sandstone and carbonate. The sandstone samples have permeability values between 170 and 500 mD, while the porosity values ranged from 19 to 32%. On the hand, the carbonates have permeability in the range of 15 and 60 mD, and porosity range from 15 to 30%. Unless otherwise stated herein, the rock samples' dimensions are: length = 7.89 cm, diameter = 3.81cm.

Properties of the rock samples are presented in Table 1, while Figures 1, 2, 3, 4, and 5 represent the rock samples, the XRD outputs for carbonate and sandstone, as well as chemical and mineral compositions of carbonate and sandstone rock samples, respectively.

Table 1: Initial physical properties of rock samples used in study.

Rock Type	Average Permeability $k_g^i(mD)$	Average Porosity $\emptyset_o$
Core plug A: Indiana limestone	16.99	15.93
Core plug B: Desert Pink Carbonate	58.90	28.43
Core plug C: Gray Berea Sandstone	174.13	19.18
Core plug D: Boise Sandstone	4523.17	31.12

Figure 1: Reservoir rock samples.

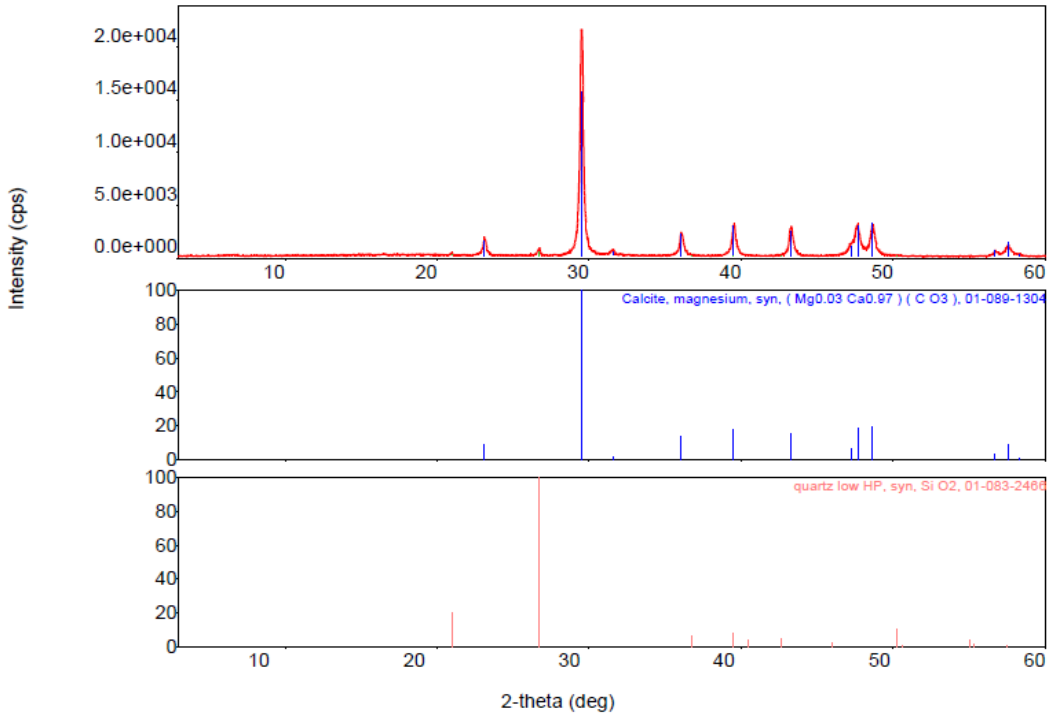

Figure 2: XRD plot for Desert Pink Carbonate.

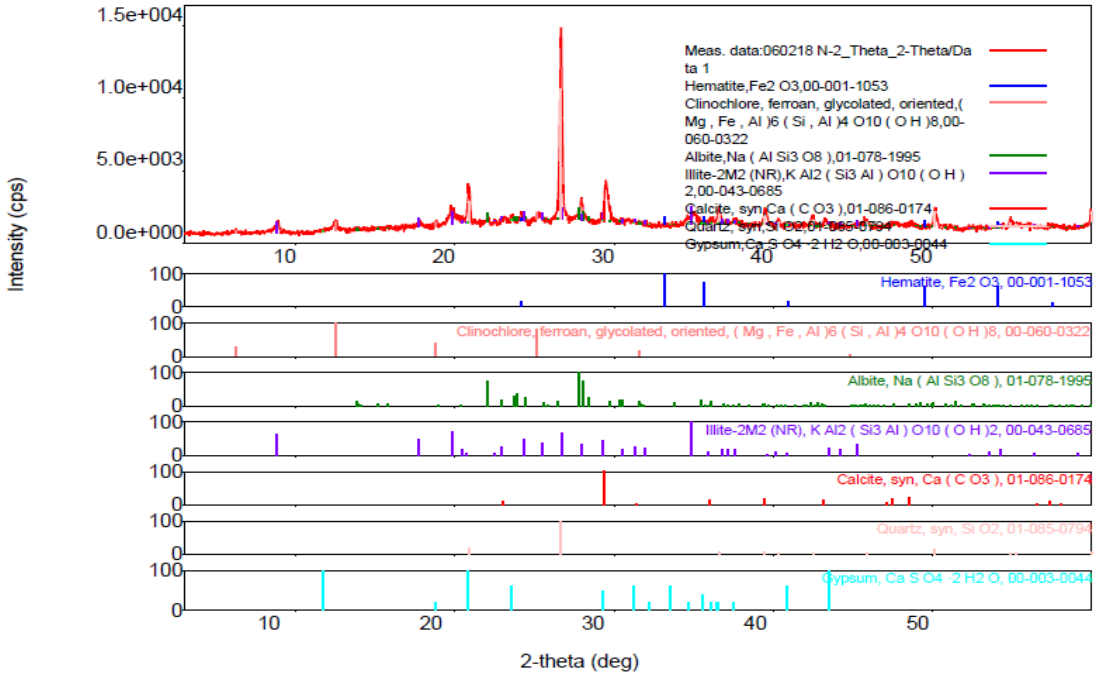

Figure 3: XRD plot for Gray Berea Sandstone.

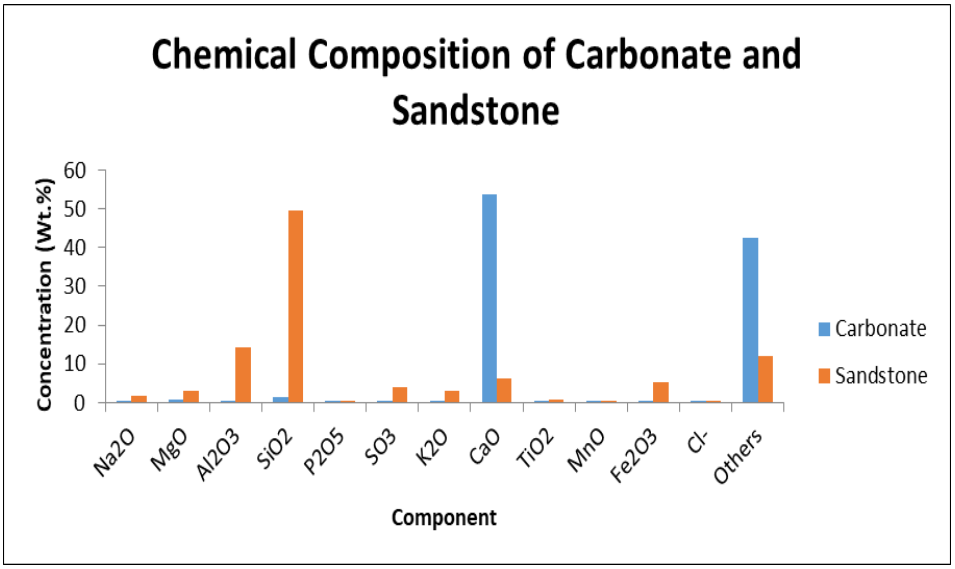

Figure 4: Chemical Composition of Carbonate and Sandstone Samples.

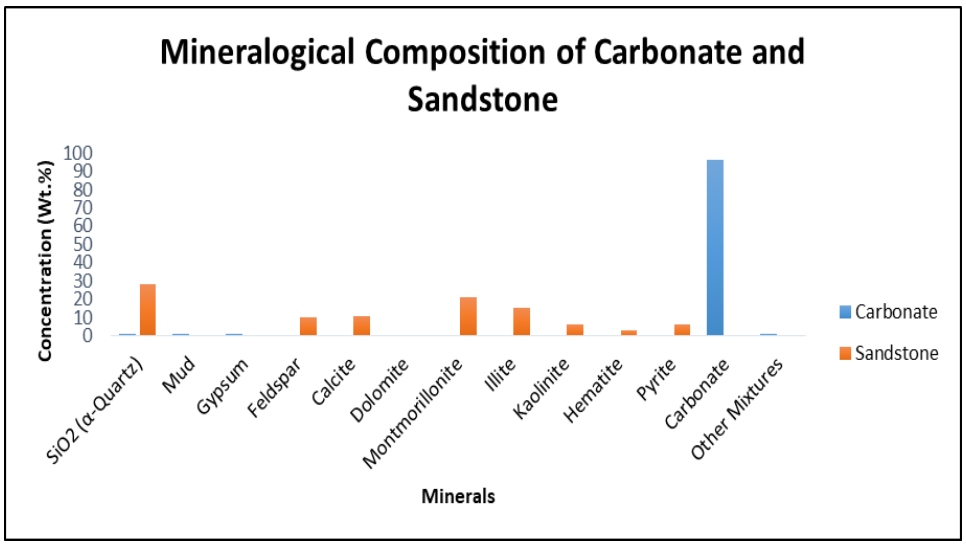

Figure 5: Mineralogical Composition of Carbonate and Sandstone Samples.

2.2 Fluids

Three different brine solutions were used in this study, namely: Sodium Chloride, NaCl; Potassium Chloride, KCl; and Caspian seawater (SW) mixed with varying amounts of NaCl salt. The constituents and physical properties of the Caspian seawater are presented in the Table 2.

The initial salt concentrations of NaCl and KCl dissolved in deionised water and seawater ranged from 10 to 200 g/mL.

Table 2: Mineral constituents and chemical properties of Caspian seawater

Cations	**mg/L**	**mg-eq/L**
Hydrogen (H^+)	5.50×10^{-9}	5.50×10^{-9}
$Na^+ + K^+$	5142	223.69
Calcium (Ca^{2+})	370	18.46
Magnesium (Mg^{2+})	6	0.49
Iron ($Fe^{2+} + Fe^{3+}$)	0.17	0.00304
Barium (Ba^{2+})	0.486	0.00
Strontium (Sr^{2+})	13.65	0.16
Anions		
Chloride (Cl^-)	6028	170.04
Bicarbonate (HCO_3^-)	470.00	7.70
Carbonate (CO_3^{2-})	15.00	0.50
Hydroxide (OH^-)	0.00	0.00
Sulphate (SO_4^{2-})	3100.00	64.57
Chemical Parameters		
Specific Gravity	1.01056	@ 20°C
Density (kg/m^3)	1008.72	@ 20°C
pH	8.26	@ 20°C
Resistivity (Ω-m)	0.5523	@ 20°C
Total Dissolved Solids (mg/L)	15150	-
Alkalinity (mg-eq/L)	8.20	-

2.3 Methodology

Each rock sample was cleaned and dried and mounted on a sleeve in a Hassler-type core holder. A confining pressure of 20 bars was applied whilst also flowing Nitrogen gas through the rock sample to measure initial gas permeability, k_g^i. The initial porosity of the rock sample was measured using Helium porosimeter. The sample was then saturated with different concentrations of NaCl, KCl, and Caspian seawater + NaCl brine solutions for 48 hours to ensure complete saturation at room temperature and atmospheric pressure conditions. At the end of the saturation stage, the fully saturated rock sample was dried in an oven at a constant temperature of 70°C for 24 hours to ensure complete drying; this was confirmed when a steady mass of the sample was recorded with regular vapour evacuation. With the completion of the rock drying, the core plug was placed in the core holder once again and Nitrogen gas flowed through to measure its new (final) permeability k_g^f, followed by a Helium porosity measurement. The procedure is repeated for all rock samples. Dry Nitrogen gas has been used in this study essentially to avoid the dissolution of CO_2 in water and consequent pH change (acidizing) that can lead to geochemical reactions and thus impact on the overall result (since the main focus of the work is to investigate only the effect of salt precipitation on permeability). Figure 6 is a schematic of the experimental set-up. Note that in this experimental investigation, only the interaction between water and dissolved ions within the porous media has been investigated, the study does not cover the oil-wet reservoir core samples.

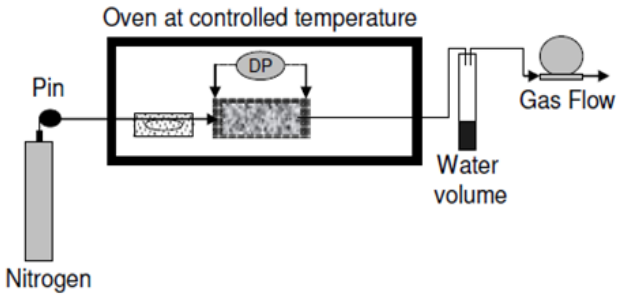

Figure 6: Experimental set-up (Adapted from Ref. [2]).

3. Results

Permeability reduction (alteration) is defined as the ratio of nitrogen gas permeability after drying in oven with the initial gas permeability, k_g^f/k_g^i. This parameter is plotted as a function of initial salt concentration (in g/L) for the different rock types as shown in the following sections.

3.1 Effect of Rock Type

The effect of rock type is depicted in Figure 7 for all 4 rock types; in Figure 7, the rock permeability alteration is plotted against initial salt concentration. Within limits of experimental error, the result from Figures 7 indicate that permeability of all 4 rock samples is altered: at 200 g/L of brine, Indiana limestone experienced about 80% permeability reduction with KCl brine compared to about 20% with NaCl brine; desert pink carbonate underwent 90% loss in permeability compared to no loss (0%) in permeability when 200 g/L of KCl and NaCl are used, respectively; the percentage decrease in permeability of Gray Berea and Boise sandstones was similar, from about 100% to 40% when saturated with 200 g/L KCl brine. The obvious trend is that permeability decreases linearly, and the most alteration occurs at a concentration of 200 g/L of KCl in Indiana limestone and desert pink carbonate rock samples.

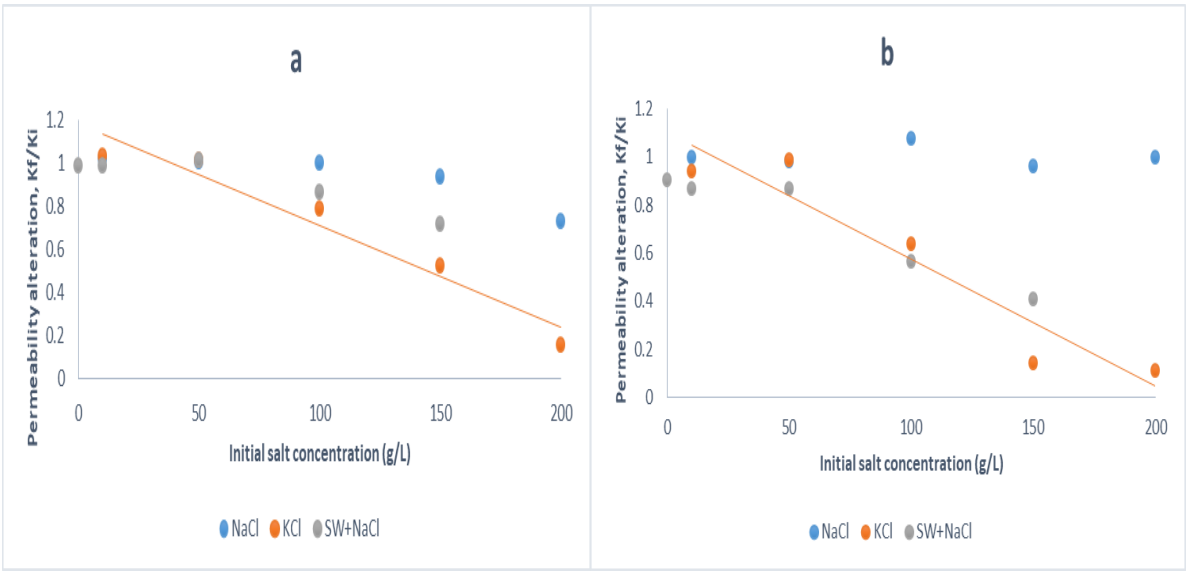

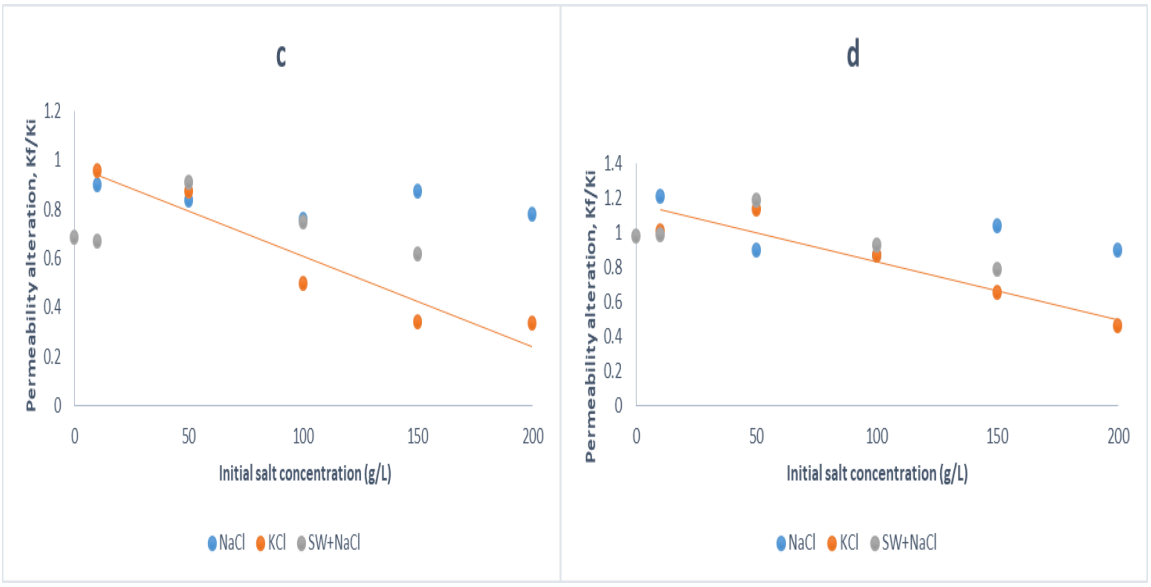

Figure 7: Permeability alteration for different rock samples at varying initial salt concentrations (a) Indiana limestone; (b) Desert pink carbonate; (c) Gray Berea sandstone; (d) Boise sandstone.

3.2 Effect of Salt Type

Figure 8 illustrates the effect of brine on the permeability alteration of the 4 rock samples. Similarly, there is a linear decline of rock permeability in all brine samples of all 3 salt types. Potassium chloride, KCl, has the most significant impact on permeability reduction of the rock samples, and this is highest in both carbonate and limestone rock samples. This is followed by the brine mixture of Caspian seawater and NaCl. NaCl is known to be more soluble in water than KCl over a wide range of temperature and pressure conditions. Therefore, the dissolution of the sodium and chloride ions could be high such that the ions are in solution and flow through the pores of the rocks. On the other hand, the potassium and chloride ions of KCl may not completely dissolve in solution and thus experience difficulty flowing through the pore throats of reservoir rock, and ultimately plug the pores and cause a decrease in the initial rock permeability. The greater implication is that with higher concentration of this salt in the brine, reservoir rock losses its ability to allow the flow of fluid through it.

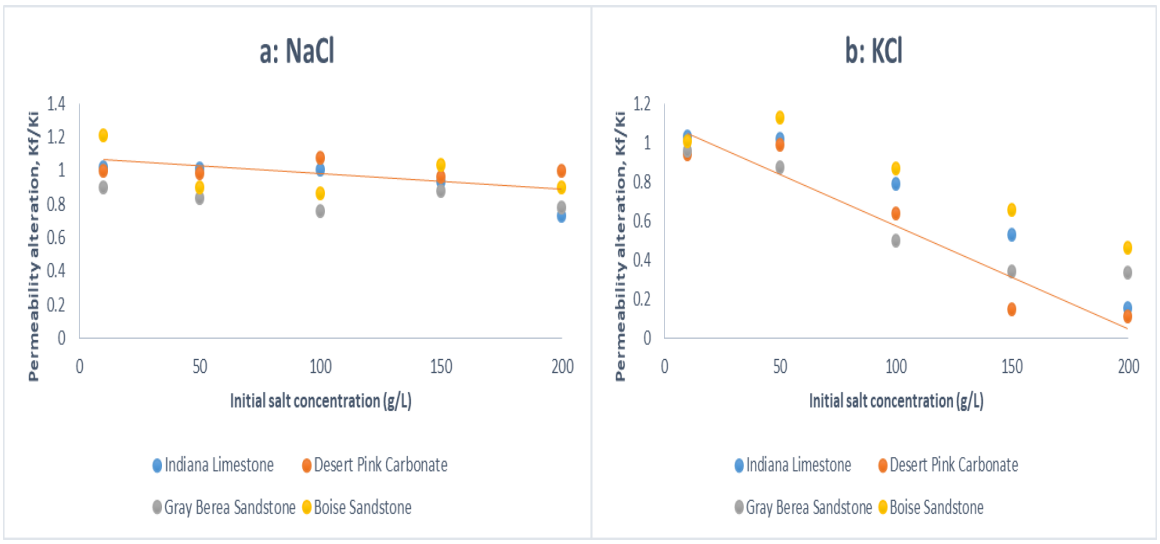

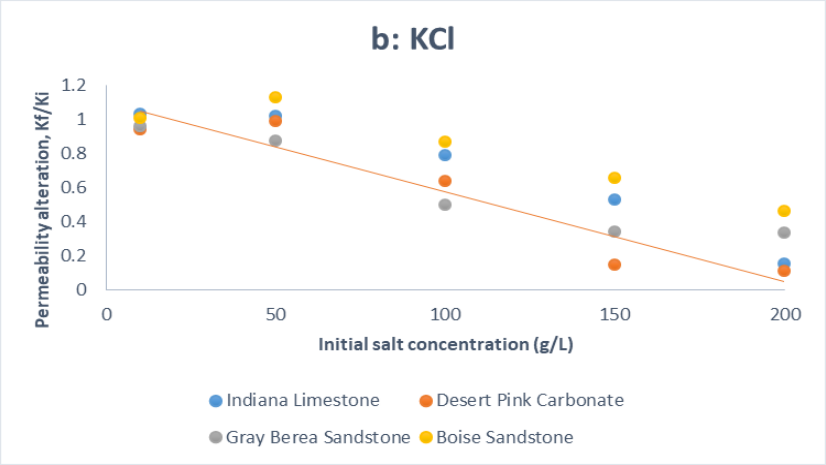

Figure 8: Permeability alteration based on the influence of the salt type; (a) NaCl; (b) KCl; (c) Seawater (SW) + NaCl.

From Figures 7 and 8, it is evident that permeability alteration depends more on the rock type than on the type of salt: limestone and carbonate rocks, with lower initial permeability values, experienced higher reduction in permeability values compared to Gray Berea and Boise sandstone samples. Note that the permeability alteration in the rock samples for NaCl brine solutions as reported in Sections 3.1 and 3.2 tended not show a continuous decrease, this is explained by the fact that the critical salt concentration (CSC) of NaCl is higher than that of KCl [16-17]. Therefore, NaCl brine should be avoided for this type of experimental investigation.

3.3 Model Based on Permeability Alteration

Assuming that the rock pore is made up of a bundle of tortuous capillary tubes, the diameter, *d*, of each tube can be expressed using the Kozeny-Carmen equation expressed in Equation (2) as:

$$d = \sqrt{32K/\emptyset_o} \ldots\ldots\ldots\ldots\ldots\ldots\ldots\ldots\ldots\ldots (2),$$

where K is permeability (millidarcy, mD), $\emptyset_o$ is initial porosity (dimensionless).

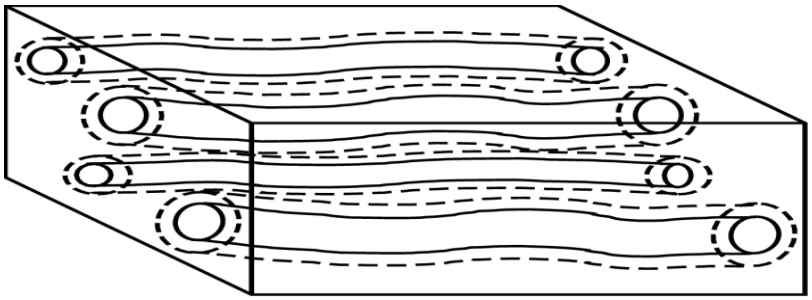

Figure 9: Model of flow path in a porous medium as a bundle of elastic capillary (Adapted from Ref. [20]).

Given the assumption that all the salt mass remains inside the porous structure of the core plugs, the total initial volume of salt in brine, which is also the total volume of precipitated salt is given in Equation (3) as:

$$V_0 = \frac{\emptyset_0 ALC_i}{\rho_s} \dots\dots\dots\dots\dots (3),$$

where A is cross-sectional area of core plug (m^2), L is length of core sample (m), C_i is initial salt concentration (g/L), ρ_s is solid salt density (kg/m^3).

This added salt volume leads to a decrease in core plug porosity, $\Delta\emptyset$, given in Equation (4) as:

$$\Delta\emptyset = \frac{\emptyset_0 C_i}{\rho_s} \dots\dots\dots\dots\dots\dots\dots (4)$$

The process of drying the salt presupposes that the entire volume of salt remains in the pores of the core plug. Since the core plug consists of capillary tubes, it is assumed that the salt mass may be deposited inside the pore structure in one of 2 main ways: in Model (a), the pores are completely filled or plugged; in Model (b), the deposition is uniform, along the interior surface of the tubes, as depicted in Figure 10.

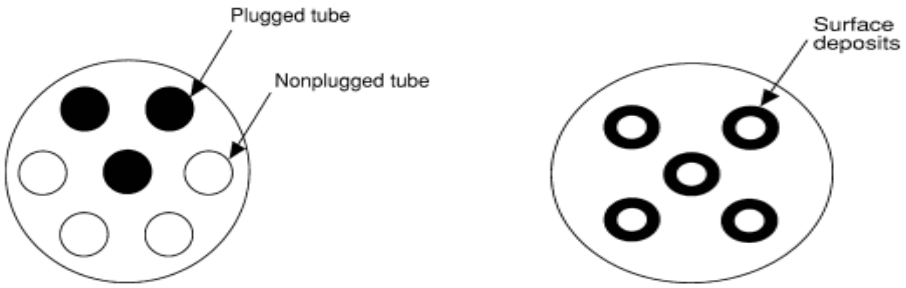

(a) (b)

Figure 10: Deposition models (a) pore-throat plugging in a core. (b) pore-surface deposition in a core (Adapted from refs. [20, [21]).

By comparing the Poiseuille's and Darcy's fluxes of the plugged capillary tubes sections, the permeability alteration equations for the 2 different deposition models are obtained:

Model (a):

$$\frac{k_g^f}{k_g^i} = 1 - \frac{C_i}{\rho_s} \dots\dots\dots\dots (5a)$$

Model (b):

$$\frac{k_g^f}{k_g^i} = \left(1 - \frac{C_i}{2\rho_s}\right)^4 \dots\dots\dots (5b)$$

It is important to stress at this point that the deposition scenario obtained from the experiments follows a linear

pattern, hence only Equation (5a) more closely predicts this deposition scenario. For KCl, whose density is ρ_s = 1980 kg/m^3, it is obvious that the alteration models [Equations (5a) and (5b)] do not adequately fit the alteration pattern obtained; the experimental alteration is larger than the model predictions, as shown by Figure 11. To understand this disparity between model and experimental results, a local investigation is undertaken.

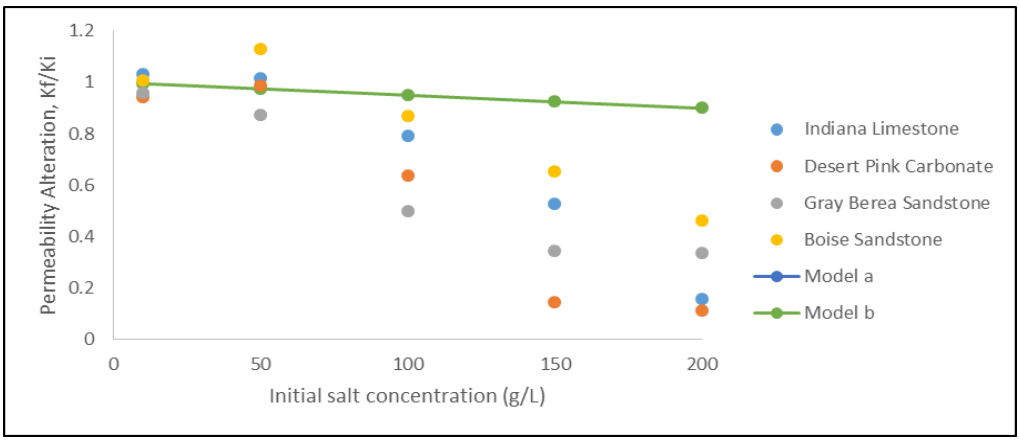

Figure 11: Permeability alteration in rock samples and models based on type of deposition of KCl salt.

3.4 Local Investigation and Convective Flux of Dissolved Salts

One of the main assumptions in this study is that deposition of the salts in the core is homogenous, i.e., salts are evenly distributed within the core. Scanning electron microscopy (SEM) analysis was performed to determine how the dissolved salts are locally distributed within the pore structure of the cores; these are presented in Figures 12 and 13. For the SEM analysis, only sample A, the Indiana limestone at 200 g/L KCl, was studied. The SEM results however indicates that the deposition of brine is not as uniform as previously assumed. In fact, the deposition of salt is non-homogeneous, though concentrated around the evaporative surfaces.

The experimental results obtained for 100 g/L, 150 g/L and 200 g/L of KCl showed very significant permeability alteration as shown in Figure 6 above. These high levels of decrease in permeability can be understood in the context of efflorescence on building stones and for diffusive drying, as pointed out by authors such as Guglielmini and his colleagues [16], Huinick and his colleagues [22], Sghair and his colleagues [23] and Peysson [15]. These authors showed that dissolved salt ions can be transported towards evaporation surfaces by convective flows induced by drying. The overwhelming conclusion from studies carried out by these authors is that the exchange of water, which then leads to evaporation, takes place at the interface, and in the case of water-wet reservoir rocks, it is the capillary force that pulls the brine to the surface [16, 22]. This leads to the accumulation of the salt at the evaporating surface. As drying continues, there is a gradual increase in brine concentration at the evaporating surface until it surpasses the solubility limit, and thus becomes precipitated as solid salt [24 , 25]. This effect is counteracted by the Fickian diffusion process that tends to homogenise the salt profile. Consequently, the Peclet number is computed, which is also defined as the ratio between the convective and diffusive flows. In this study, while operating the oven at constant temperature of 70^{o}C and with a drying time of 24 hours, the Peclet number and mean drying rates for all 4 samples are calculated and presented in Table 3. For all 4 rock samples saturated with 200 g/L KCl brine, the Peclet number, *Pe* is significantly greater

than 1, i.e., (*Pe>>1*). This confirms the fact that the drying process and flow regime is convective in nature and salt deposition is non-homogeneous, and it is tnear the evaporating surface. The white spots and patches in Figure 12 (b) are the solid KCl in the rock pores.

Table 3: Peclet number calculations for all 4 rock samples.

Rock sample	Water Saturated mass (g)	Mean Drying rate (g/s)	h ($m^3/m^2.s$)	Peclet Number, *Pe*
Indiana Limestone	184.75	1.11×10^{-3}	9.45×10^{-8}	25.39
Desert Pink Carbonate	172.71	1.59×10^{-3}	1.36×10^{-7}	20.39
Gray Berea Sandstone	149.57	1.31×10^{-3}	1.12×10^{-7}	24.92
Boise Sandstone	128.65	2.10×10^{-3}	1.79×10^{-7}	24.67

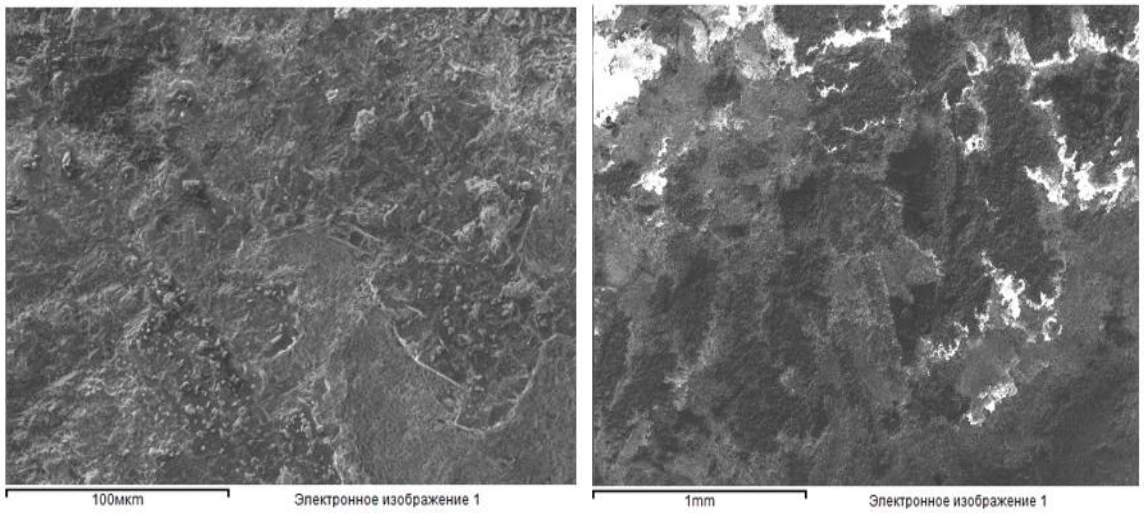

(a) **(**b**)**

Figure 12: SEM image of Indiana limestone: (a) initial dry state, (b) after KCl salt precipitation.

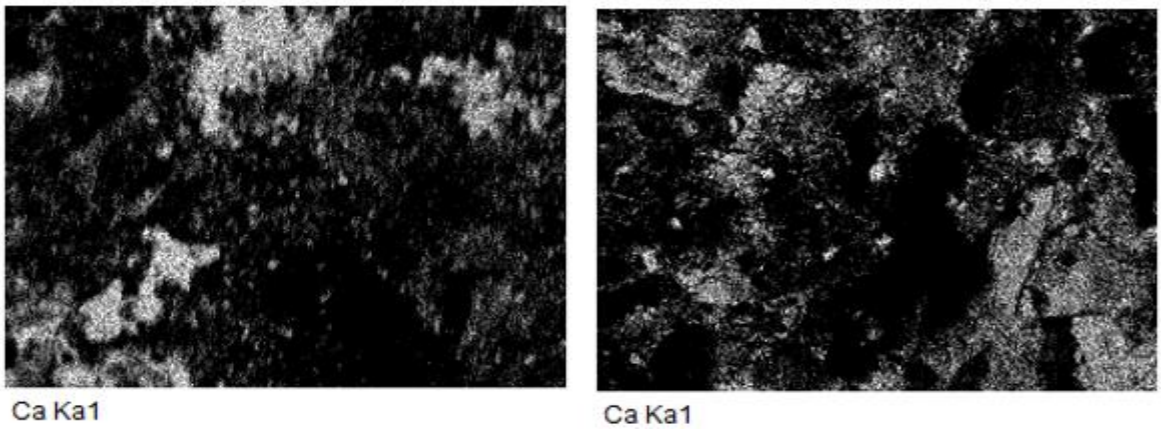

Figure 13: SEM image of spatial distribution of KCl salts in Indiana limestone.

4. Model Update

Since the proposed models are not fully able to depict the appropriate plugging mechanism occurring inside the pore spaces of the reservoir rock, the question that readily comes to mind would be '*why the non-conformity between experimental results and proposed model*?' To model the actual plugging scenario and permeability alteration based on experimental results, a modification of Equation (5a) is proposed. This is achieved by introducing an alteration parameter, which expresses the ratio of the length of the core actually plugged, l, compared to entire length of core, L; the parameter is expressed as $\gamma = l/L$, and introduced into the second term of the left-hand side (LHS) of Equation (5a) to give Equation (6):

$$\frac{k_g^f}{k_g^i} = 1 - \frac{C_i}{\gamma \rho_s} \ldots\ldots\ldots\ldots (6)$$

Equation (6) indicates that the permeability reduction is dependent on how much of the capillary tube is filled with brine salts through deposition compared to how much tube space was initially available in the core plug. Figure 14 shows the comparison between the experimental results, model results based on Equation (5a) and the updated model based on Equation (6) (known as *Updated Model*), for deposition of KCl brine at different initial salt concentrations. The fairly good agreement of these results are for alteration parameters, γ, of 14%, 13%, 14% and 19%, for Indiana limestone, desert pink carbonate, Gray Berea sandstone, and Boise sandstone, respectively. This shows that the plugging of the core plug with KCl brine salt only occurs in up to about 1/5th (20%) of the entire core plug volume.

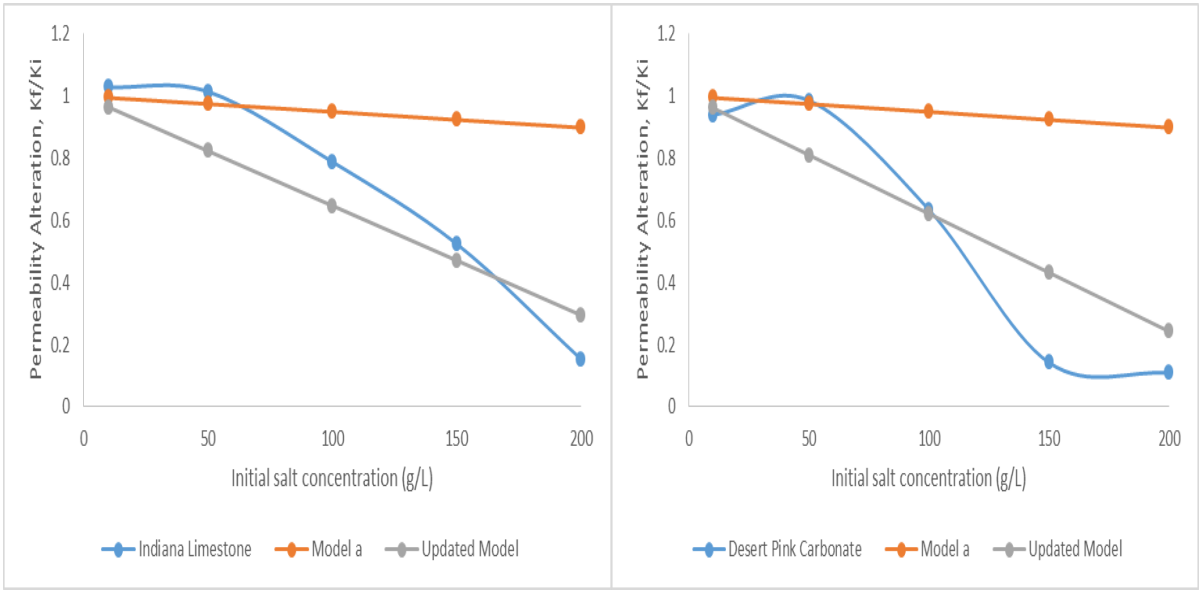

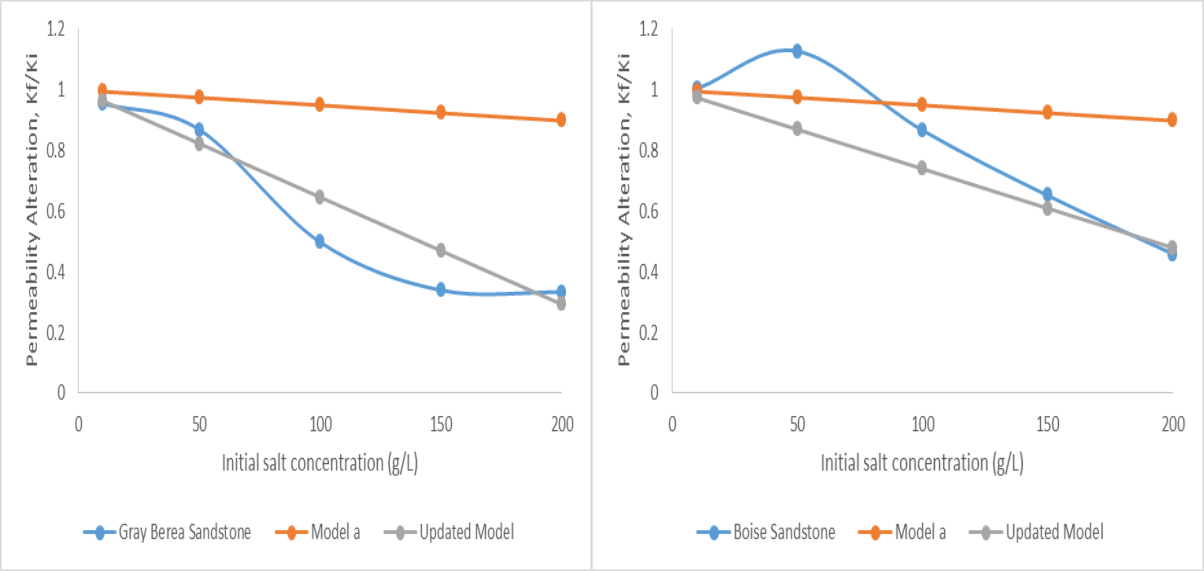

Figure 14: Experimental permeability alteration for 4 rock samples and comparison with linear Model a and Updated Model based on the alteration parameter.

5. Conclusion

The injection of CO_2 into saline aquifers will bring about a wide variety of complex processes, the most common being the dry-out of the formation particularly around the injection well. This is of utmost concern because it may induce precipitation of residual brine, with consequent loss of porosity, permeability and injectivity. In this study, permeability impairment of 4 different rock samples was experimentally investigated; these rock samples possess properties that are typical of those used in CO_2 sequestration, with 3 different brine solutions. An overall linear decrease in permeability was observed in all the samples and the alteration was most severe in desert pink carbonate rock when saturated with KCl.

Although the 2 models proposed based on the Poiseuille and Darcy's flux under-predicted the level of permeability alteration, an updated model was proposed that captured the alteration pattern closely. SEM analysis of the rock sample shows that the salt precipitation is driven by convective flux and typically occurs around the evaporative surface of the sample, and that the reservoir rock pores are plugged by the solid salt crystals formed as a consequence. The study also demonstrated that salt precipitation profiles are usually not homogeneous; they tend to occur around the injection and evaporative surfaces, through a convective mechanism, evidenced by the significantly high Peclet number (Pe >>1).

Given the findings from this research, it is fair to say that in carbon capture and storage (CCS) injection wells, where the host rock is already saturated with some amount of dissolved salts (brine), the observed convective evaporative mechanism in this study is likely to occur, which could then lead to the deposition of salts around the injection well, and its subsequent plugging, ultimately leading to a decrease in initial rock permeability. In addition to loss of permeability, the host rock may also suffer from loss of porosity and difficulty with injectivity, all of which lead to increased pumping cost for a typical CO_2 sequestration project. Therefore, for all future gas storage application in saline aquifiers, the risk that reduced injectivity from permeability alteration

poses should be exhaustively investigated. Salting out is a very important issue that should be considered for future storage application in saline aquifers and the experimental investigation undertaken in this study clearly show that permeability alteration is a potential risk that should be studied in great detail due to the consequences in terms of injectivity.

It should be noted while this study can be extended to oil-wet reservoir rock samples, this particular experimental investigation however has focussed only on water and a compressible displacing medium (nitrogen gas).

Acknowledgement

The authors wish to thank Mr Kamal Mustafayev of Azlab LLC and his colleagues for their diligence, patience, and professionalism in performing the experiments. Special thanks also to an anonymous reviewer for his time in proof-reading and critiquing the work, which helped to further improve the quality of the research.

6. Conflict of Interest Statement

The authors declare that there is no conflict of interest.

References

[1] https://www.iea.org/publications/freepublications/publication/GECO2017.pdf (Accessed on 15th September, 2018).

[2] Peysson, Y., Bazin, B., Magnier, C., Kohler, E., Youseff, S., 2011: Permeability Alteration due to Salt Precipitation driven by Drying in the Context of CO_2 Injection; *Energy Procedia*, 4, 4387 – 4394.

[3] Zeidoni, M., Pooladi-Darvish, M., Keith, D., 2009: Analytical Solution to Evaluate Salt Precipitation duding CO2 Injection in Saline Aquifers; *International Journal of Greenhouse Gas Control*, 3, 600 – 611.

[4] André, L., Azaroual, M., Peysson, Y., Bazin, B., 2011: Impact of Porous Medium Desiccation during Anhydrous CO_2 Injection in Deep Saline Aquifers: Up Scaling from Experimental Results at Laboratory Scale to Near-Well Region; *Energy Procedia*, 4, 4442- 4449.

[5] Rufai, A., Crawshaw, J., 2017: Micromodel Observations of Evaporative Drying and Salt Deposition in Porous Media; *Physics of Fluids*, 29, 126603.

[6] Madhadevan, J., Sharma, M.M., Yortsos, Y.C., 2006: Water Removal from Porous Media by Gas Injection: Experiments and Simulation; Transp Porous Media, 66, 287-309

[7] Allerton, J, Brownell, L.E., Katz, D.L., 1949: Through-drying of Porous Media; Chem. Eng. Prog., 45(10), 619-635

[8] Yiortis, A.G., Boudouvis, A.G., Stubos, A.K., Tsimpanogiannis, I.N., Yortos, Y.C., 2004: The Effect of Liquid Films on the Drying of Porous Media; AIChE Journal, 50.

[9] Luikov, A.V., 1966: Heat and Mass Transfer in Capillary Porous Media; Pergamon Press, London, UK.

[10] Whitaker, S., 1977a: Simultaneous Heat, Mass and Momentum Transfer in Porous Media. A Theory of Drying. Advances in Heat Transfer, 1(13), 119 – 203

[11] Whitaker, S., 1977b: Toward a Diffusion Theory of Drying; Industrial Engineering Chemistry Fundamentals, 16(4), 408 – 414.

[12] Pruess, K., Muller, N., 2009: Formation Dry-Out from C02 Injection into Saline Aquifers: 1. Effects of Solid Precipitation and their Mitigation; Water Resources Research, 45, W03402

[13] Giorgis, T., Carpita, M., Battistelli, A., 2007: 2D Modelling of Salt Precipitation during the Injection of Dry C02 in a Depleted Gas Reservoir; Energy Conservation and Management, 48, 1816 – 1826

[14] Nadeau, J.P., Puiggali, J.R., 1995: Drying – From Physical Properties to Industrial Processes (in French); Tec & Doc Lavoisiers, Paris.

[15] Peysson, Y., 2012: Permeability Alteration Induced by Drying of Brines in Porous Media; *The European Physical Journal Applied Physics*, DOI: 10.1051/epjap/2012120088.

[16] Guglielmini L., Gontcharov A., Aldykiewicz Jr., Stones H.A., 2008: Drying of Salt Solutions in Porous Materials: Intermediate-Time Dynamics and Efflorescence, *Physics of Fluids*, 20, 077101.

[17] Pel, L., Huinink, H., Kopinga, K., 2003: Salt Transport and Crystallization in Porous Building Materials; Magn. Reson. Imaging, 21, 317.

[18] Abrams, A., Vinegar, H.J., 1985: Impairment Mechanisms in Vicksburg Tight Gas Sands, Paper 13883 presented at the Society of Petroleum Engineers/Department of Energy Low Permeability Gas Reservoirs Conference held in Denver Colorado.

[19] Peters, E.J., Hardham,W.D., 1990: Visualisation of Fluid Displacements in Porous Media using Computed Tomography Imaging; J.Pet. Sci. Eng., 4, 155 – 168

[20] Civan, F., 2018: Stress Dependency of Permeability Represented by an Elastic Cylindrical Pore-Shell Model: Comment on Zhu et al; *Transport Porous Media*, 122: 235 – 252.

[21] Civan, F., 2007: Reservoir Formation Damage: Fundamentals, Modelling, Assessment and Mitigation, 2nd ed., Gulf Professional Publishing, Oxford, UK, 263 p.

[22] Huinink H.P., Pel L., Michels M.A.J., 2002: How Ions Distribute in a Drying Porous Medium: A

Simple Model, *Physics of Fluids*, 14-4, p.1389-1395.

[23] Sghair, N., Prat, M., Ben Nasrallah, S., 2007: On Ions Transport during Drying in a Porous Medium, *Transport Porous Media*, 67, 243-274.

[24] Bacci, G., Korre, A., Durucan, S., 2011: Experimental Investigation into Salt Precipitation during CO_2 Injection in Saline Aquifers, *Energy Procedia* **4**, 4450–4456.

[25] Wang, Y., Mackie, E., Rohan, J., Luce, T., Knabe, R., Appel, M., 2009: Experimental Study on Halite Precipitation during CO_2 Sequestration, in *International Symposium of the Society of Core Analysts Held in Noordwijk, The Netherlands* (The Society of Core Analysts), pp. 27–30.